Go Real: Power Electronics from Simulations to Experiments in Hours

Qing-Chang Zhong, Yeqin Wang, Yiting Dong, Beibei Ren, and Mohammad Amin

***Abstract*—The only constant is change. Power systems worldwide are going through a paradigm change from centralization generation to distributed generation; transportation systems are being electrified; and billions of lives in third-world countries are awaiting low-cost sustainable electricity. Control and power electronic technologies are two common enablers to address these grand challenges. Empowering next-generation engineers with hands-on skills in control and power electronics has become a priority for global higher education. However, setting up a suitable experimental system requires time, effort, and a broad range of expertise. This paper aims to help researchers, university professors, graduate students, engineers, and startups remove the barriers to go real from simulations to experiments for various power electronic systems and improve the efficiency and productivity of research and education. It shows that it is possible to obtain experimental results within hours after completing simulations by adopting the SYNDEM Smart Grid Research and Educational Kit, which is a reconfigurable, open-source, multifunctional power electronic converter with the capability of directly downloading codes from Matlab/Simulink. This will minimize the time, cost, and efforts needed to develop hardware systems and to program control algorithms. At first, the Kit will be introduced, with sample topologies highlighted. Then, two sample case studies will be described. In one case, the Kit is configured as a DC-DC-AC converter to implement an integrated PV-storage system. In the other case, the Kit is configured as an AC motor drive. Experimental results are presented for both cases.**

I. Introduction

Control and power electronics are two major enablers for the paradigm shift of power systems from centralized generation to distributed generation, the electrification of transportation, and the transformation of billions of lives in third-world countries. For power systems or smart grids, a large number of active units including wind farms, solar farms, DERs, electric vehicles, energy storage systems and flexible loads are being integrated into power systems through power electronic converters [1], [2]. This imposes great challenges to the stability, scalability, reliability, security and resiliency of future power systems. Hence, it is vital to develop appropriate control architecture and technologies so that all these different players are able to take part in the regulation of future power systems. For electrification of transportation, power electronic converters are widely used in more-electric aircraft, all-electric ships, electric vehicles, spaceships, and satellites etc. In third-world countries, billions of lives are waiting for low-cost solutions to provide electricity. The control of power electronic converters lies in the heart of these applications and many other areas such as computers, telecommunication, data centers, consumer electronics, lighting, motor drives etc.

While advancing technologies for these applications is important to address the problems, another key is to provide low-cost versatile tools to facilitate the research and development of technologies and to educate next-generation engineers. A lot of education and training on control of power electronics are simulation-based because of the lack of affordable and reconfigurable hardware platform. The emerging of hardware-in-the-loop (HIL) simulation has made it easier to obtain simulation results that are close to real experiments. However, the price of hardware-in-the-loop simulation systems is still high. While these simulations reflect the behavior of real systems to some extent, many practical issues cannot be accurately modeled or studied with simulations. Needless to say, real experiments are the best way to reflect the dynamics and characteristics of real applications and carrying out physical experiments should be an integrated part of training next-generation power electronics engineers and leaders. In order to make this happen, two major challenges need to be overcome: the availability of suitable hardware platforms and the elimination of software coding burden. It usually takes several months for a skilled person to build up an experimental system after several iterations. Furthermore, different topologies usually require different new hardware designs. As to software coding, it is often the job of another person – it is difficult for a hardware engineer to write codes. It often takes several months or longer for a beginner to fully understand the programming platform and the target machine. Moreover, code debugging can be very time-consuming. This is particularly true for the control community because of the strengths on developing control algorithms and, relatively, the lack of hardware and software skills.

This demonstration session aims to help researchers, graduate students, and engineers remove the barriers to carry out physical experiments for control of power electronic-based systems. It will demonstrate that it is possible to obtain experimental results within hours after completing simulations by adopting the SYNDEM Smart Grid Research and Educational Kit, which is a multifunctional, reconfigurable, and open-source power electronic converter with the capability of directly downloading codes from Matlab/Simulink. As a result, the two major challenges mentioned above are overcome. In this session, the Smart Grid Research and Educational Kit and its unique features will be presented, together with sample case studies.

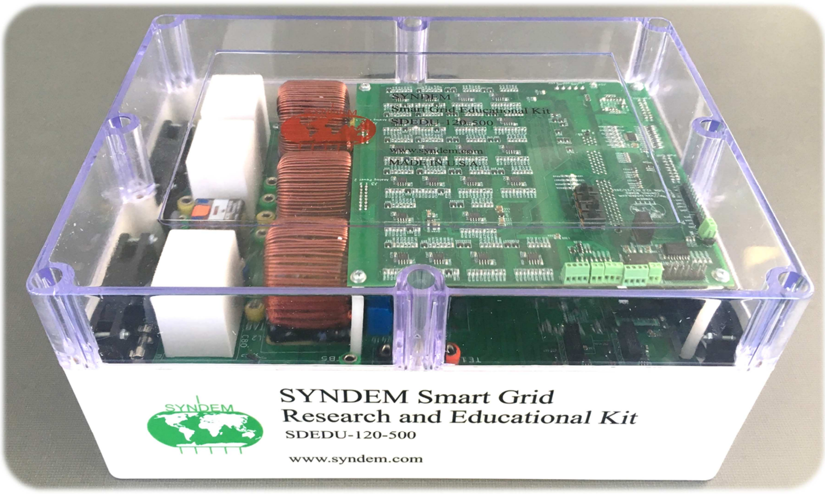

Fig. 1. SYNDEM Smart Grid Research and Educational Kit

II. SYNDEM Smart Grid Research and Educational Kit

A. Overview

The Kit is featured by MathWorks® as a reconfigurable power electronic converter for research and education in smart grids[1]. The Kit can be reconfigured to obtain 10+ different power electronic converters, covering DC/DC converters and single-phase/three-phase DC/AC, AC/DC, and AC/DC/AC converters. As a result, it can be used to quickly set up research, development, and education platforms for different applications, such as solar power integration, wind power integration, machine drives, energy storage systems, and flexible loads. Moreover, there is no need to spend time on coding because it adopts the widely-used Texas Instrument (TI) C2000 ControlCARD and is equipped with the automatic code generation tools of MATLAB®, Simulink®, and TI Code Composer Studio™ (CCS), making it possible to generate experimental results within hours from simulations. It comes with complete interface details and sample implementations, based on which users can easily test their own control algorithms.

The main features of the Kit include

- Reconfigurable to obtain 10+ different power electronic converter topologies;
- Capable of directly downloading control codes from Matlab/Simulink;
- Ideal for research in smart grid, microgrid, renewable energy, EV, energy storage etc.;
- Compatible with utilities around the world with 120 V or 230 V voltage, 5A current;
- Versatile communication interfaces, such as RS485 and CAN, for SCADA;
- Multiple DAC channels for easy debugging and monitoring of internal states;
- Suitable for parallel, grid-tied, or islanded operation with single or multiple kits.

[1] https://www.mathworks.com/products/connections/product_detail/syndem-smart-grid-kit.html

B. Hardware Structure

Each Kit consists of one control board and up to two power boards. Figure 1 shows a picture of the Kit with one power board. The control board is on top of the power board and auxiliary power supplies are located beneath the power board. The Texas Instrument (TI) C2000 ControlCARD is inserted at the back of the control board. The control board has four switches for users to define the functions.

Power Board: The power board contains a three-leg IGBT module A1P35S12M3 and its driver circuits, relay, jumper wire connectors, current sensors, voltage sensors, inductors, capacitors, and fuses. The diagram of the main power circuit is shown in Figure 2. The power board accepts PWM signals from the control board through J7/J4 and transfers analogue voltage/current signals to the control board through J2/J3. The IGBT module A1P35S12M3 contains six 1200V 35A devices in three legs with a common positive bus. It has a built-in NTC temperature sensor for thermal protection. There are two DC-bus 470μF 450 V capacitors, $C76$ and $C77$, which can be configured in series or in parallel to meet the requirement of the voltage rating or the capacitance. There are three sets of inductors $L1$, $L2$, and $L3$ and capacitors $C78$, $C79$, $C80$, with two sets reconfigurable. Moreover, inductor $L2$ and Capacitor $C78$ can be placed freely. A relay is included to facilitate grid connection. All the inductor currents and capacitor voltages as well as the DC-bus current and voltage are measured and sent to the control board. In addition, two voltages on the grid side are measured to facilitate grid connection. The power board is also equipped with AC fuses $F2$, $F3$, and $F4$, DC fuse $F1$, NTC thermistors VR1, VR2, and VR3 for protection and a pre-charging resistor $R61$. The power board is also equipped with a standalone 1600 V 35 A three-phase diode bridge with a 470μF 450 V capacitor, making it possible to power the DC bus from an external transformer.

Control Board: The control board includes a Texas Instrument (TI) C2000 TMS320F28335 ControlCARD, signal conditioning circuits for AC signals, 22-channel 12 bit ADC, 4-channel 12 bit DAC, 4 switches, 4 LEDs, SPI, RS485 and

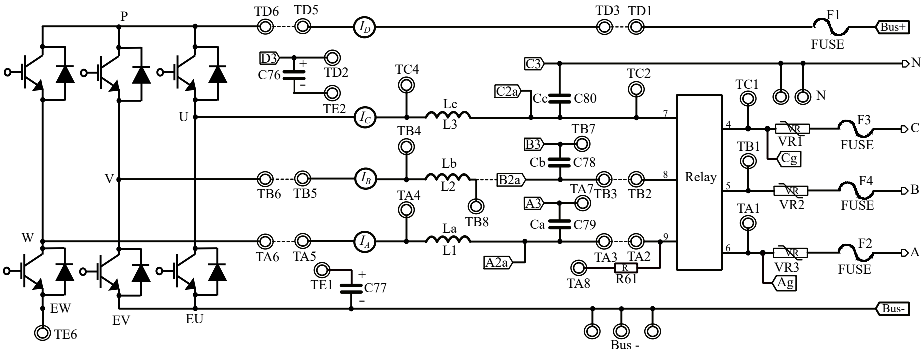

Fig. 2. SYNDEM Smart Grid Research and Educational Kit: Main power circuit

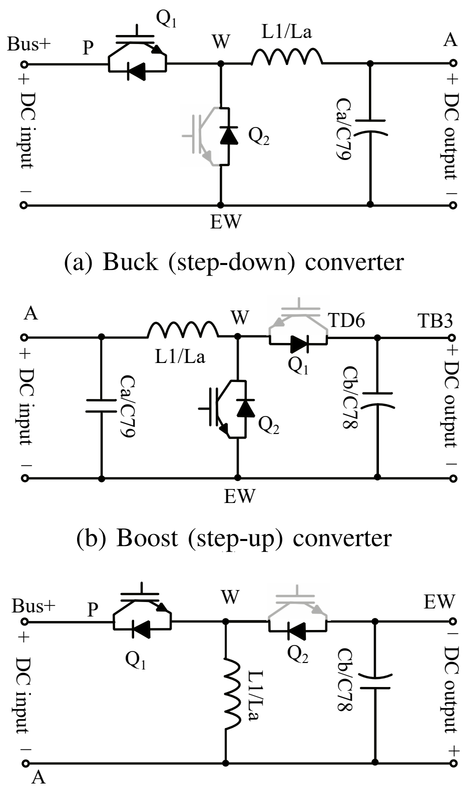

(a) Buck (step-down) converter

(b) Boost (step-up) converter

(c) Buck-boost converter

Fig. 3. Implementation of DC-DC converters

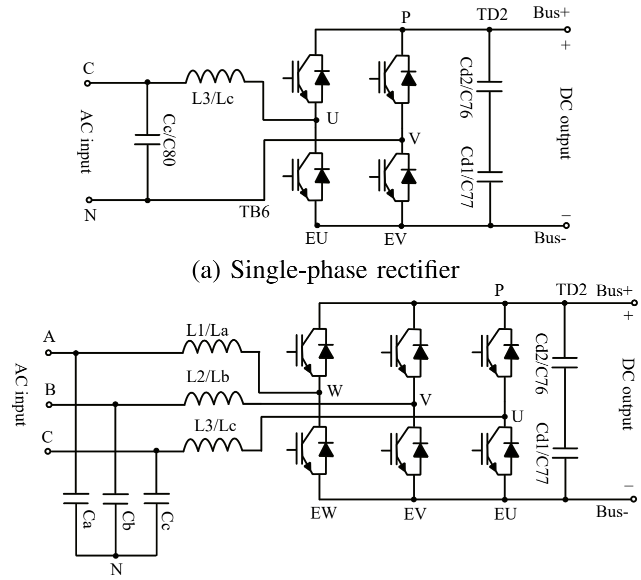

(a) Single-phase rectifier

(b) Three-phase rectifier

Fig. 4. Implementation of PWM-controlled rectifiers

CAN interfaces, protection circuits, and PWM circuits. Up to two power boards can be connected to one control board. This makes it possible to carry out experiments for two three-phase converters with one controller, e.g., the back-to-back converters in PMSG and DFIG WPGS.

C. Sample Conversion Topologies

The Kit can be reconfigured into different converter topologies for various applications, such as solar power, wind power, energy storage system, motor drives, electric vehicles, and flexible loads. Some sample topologies are outlined below.

DC-DC Converters: DC-DC converters are used to change the voltage level of a DC source to another level that is suitable for the load connected. A DC-DC converter can be designed to increase the voltage, decrease the voltage, or both. The ratio between the output voltage and the input voltage is called the conversion ratio. When the conversion ratio is lower than 1, the converter is called a buck (step-down) converter; when the conversion ratio is higher than 1, the converter is called a boost (step-up) converter; when the conversion ratio can be higher and lower than 1, then the converter is called a buck-boost converter. The SYNDEM Kit can be adopted to realize all these three types of DC-DC converters. Figure 3 shows some implementations.

PWM-controlled Rectifiers: The SYNDEM Kit can be configured to form a single-phase or three-phase PWM-controlled rectifier, as shown in Figure 4. The circuit configurations of these PWM-controlled rectifiers can also be used for single-phase/three-phase uncontrolled rectifiers, with the main difference being that the switches are not controlled through PWM signals from the DSP.

θ-converters: The SYNDEM Kit can be used to implement other rectification topologies, for example, the θ-converter proposed in [3]. The configuration of the θ-converter is shown in Figure 5, which is a single-phase bridge converter that looks

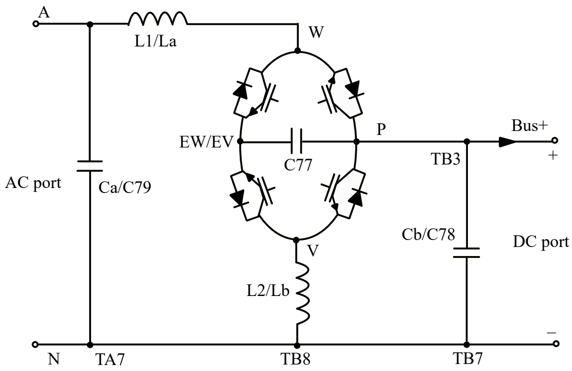

Fig. 5. Implementation of the θ-converter

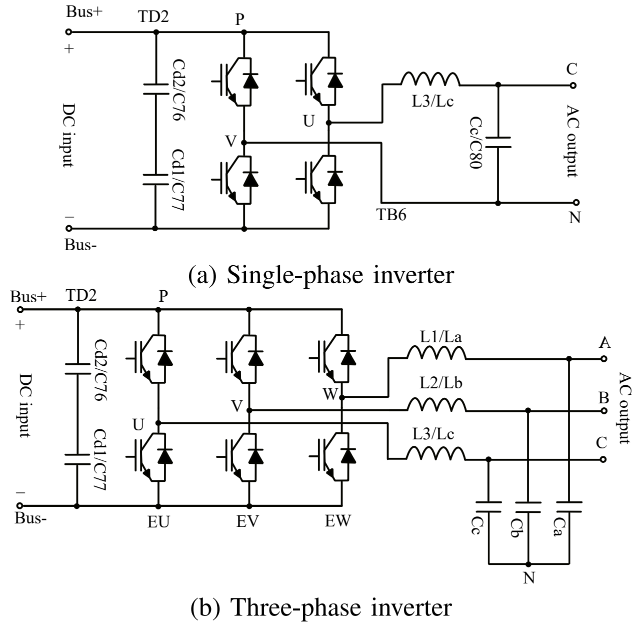

Fig. 6. Implementation of inverters

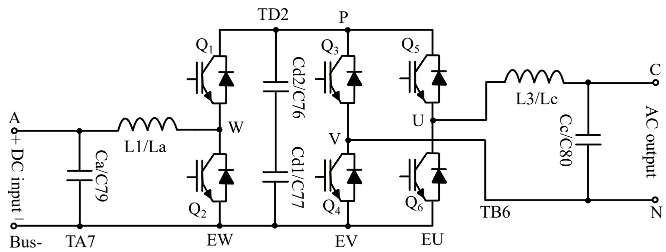

Fig. 7. Implementation of a DC-DC-AC converter

like the symbol θ. It has a common AC and DC ground, which reduces common-mode voltages and leakage currents. The DC-bus capacitor $C77$ provides a direct path for the double-frequency ripple current inherently existing in single-phase converters to return continuously. The output capacitor $C78$ only deals with switching ripples so it can be chosen small. Moreover, the DC-bus capacitor $C77$ is designed to store the system ripple energy with large voltage ripples. As a result, its capacitance can be reduced as well. The θ-converter offers more advantages than a conventional bridge converter because its two legs are controlled independently; see [3] for details. The inductor $L2/Lb$ can also be connected between P and Bus+ to form an improved θ-converter.

Inverters: An inverter converts an DC source into an AC output. According to the type of the DC supply, there are current-source inverters (CSI) and voltage-source inverters (VSI). Typically, an inverter is a VSI if there is a large capacitor across the DC bus and is a CSI if there is a large inductor in series with the DC supply. The SYNDEM Kit can be configured as VSI for single-phase and three-phase applications, as shown in Figure 6. Depending on the control algorithm implemented, the output of the inverter can be current-controlled or voltage-controlled. Both control methods can be implemented with the SYNDEM Kit because there are sensors to measure the output voltage and the output current. The inverter can be operated in the islanded mode or in the grid-connected mode. If it is operated in the grid-connected mode, the voltage on the grid side is available for synchronization. Once it is synchronized, the relay can be turned ON.

DC-DC-AC Converters: Some applications require DC-DC and DC-AC two-stage conversion. For example, a solar power system often needs a DC-DC converter on the PV side to step up the voltage before conversion into AC with a DC-AC converter. The SYNDEM Kit can be configured to implement this DC-DC-AC conversion, as shown in Figure 7. Two separate controllers but inside the same ControlCard are needed for the DC-DC converter and the DC-AC inverter, respectively.

Single-phase AC-DC-AC Back-to-Back Converters: The SYNDEM Kit can be used to implement AC-DC and DC-AC back-to-back conversion. As shown in Figure 8, the implementation only needs three legs, with a common neutral point provided by the θ-converter. The three legs are controlled independently.

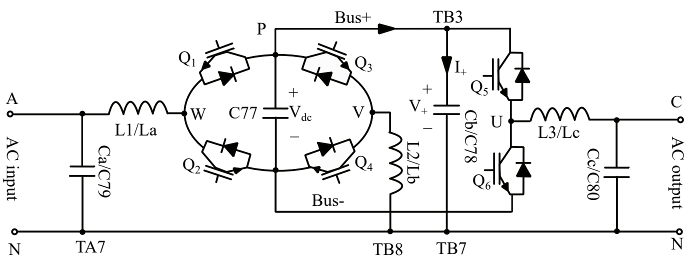

Fig. 8. Implementation of a single-phase back-to-back converter

Three-phase AC-DC-AC Back-to-Back Converters: Three-phase applications, such as wind power systems, frequency converters, and machine drives, often require three-phase back-to-back converters. One SYNDEM Kit plus an additional power board can be used to form such a three-phase back-to-back converter, as shown in Figure 9. Both power boards can be controlled through one control board.

III. Sample Case Studies

A. AC Motor Drive

The system setup for AC motor drive based on a permanent magnet synchronous motors (PMSM) system is shown in

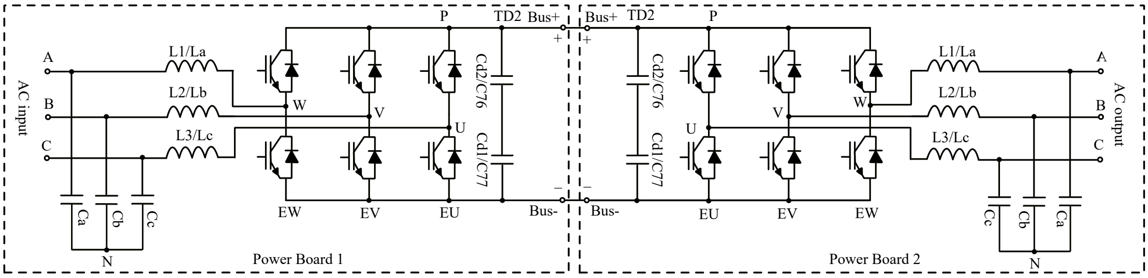

Fig. 9. Implementation of a three-phase back-to-back converter

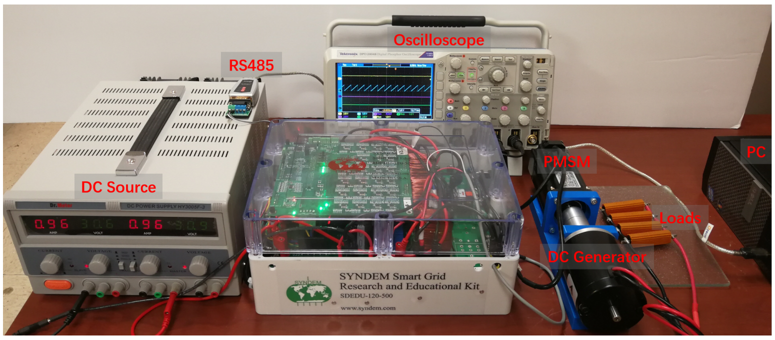

Fig. 10. AC motor drive for a PMSM system through the SYNDEM Kit

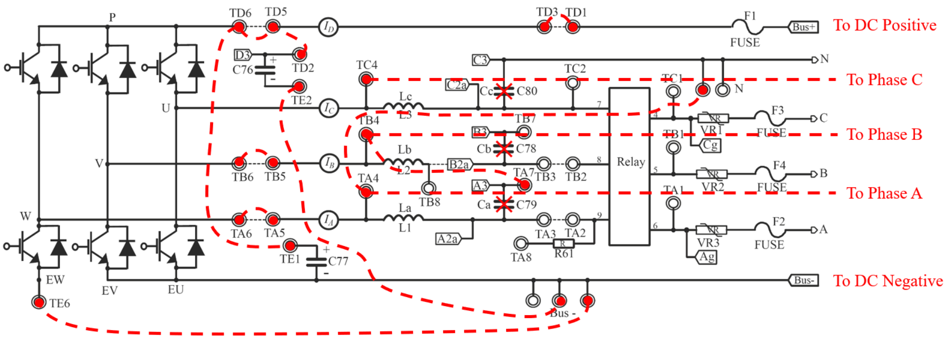

Fig. 11. The wire configuration of main power circuit for the PMSM drive

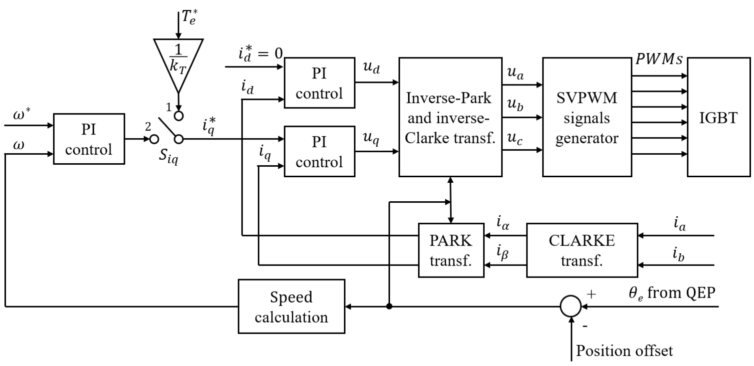

Fig. 12. Vector control of the PMSM through either torque control or speed control

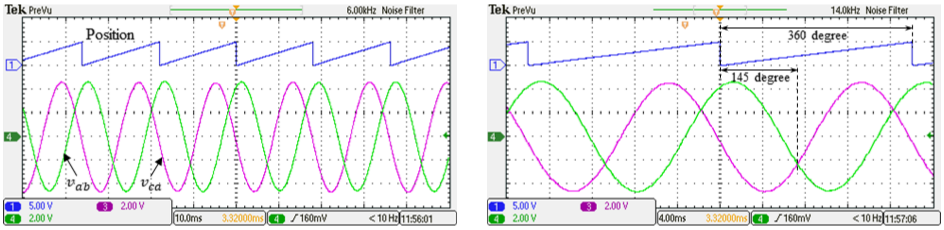

(a) Rotor position versus v_{ab} and v_{ca} (b) Zoom-in results

Fig. 13. Initial rotor position calibration through the back-EMF of a PMSM

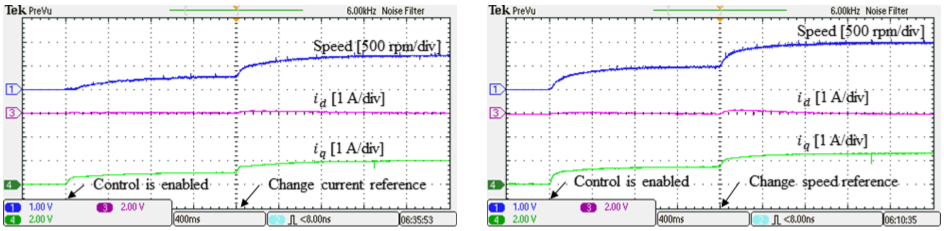

(a) Case II: Torque control (b) Case III: Speed control

Fig. 14. Experimental results of AC motor drive

Figure 10, where a SYNDEM kit is configured as a three-phase motor controller to drive an Anaheim Automation EMJ-04 PMSM. A 60 V DC source is used to supply DC power for the SYNDEM Kit. An AmpFlow E30-150 DC generator plus four parallel-connected resistors (total 0.25 Ω) are performed as the mechanical load for the PMSM. An oscilloscope is used to monitor and record system operation date through the DAC outputs from the SYNDEM kit, and further data can be monitored through RS485 communication between the SYNDEM Kit and PC.

The wire configuration of the main power circuit for the PMSM drive is shown in Figure 11, where, unlike the applications on power converters, the *LC* filters based on the inductors and AC capacitors are not required for motor drive. In order to remove the effects from the AC capacitors for the back EMF measurements during initial rotor position calibration, three AC capacitors, C_a, C_b, and C_c, are customized to be not soldered. The PMSM is directly connected to three outputs of the IGBT module after the current sensors. The back EMFs of line-line voltages v_{ab} and v_{ca} can be measured through sensing points between A2a and A3, and between C2a and C3, respectively. The inductors does not affect the voltage measurement, because there are no currents passing through them. And two DC capacitors are parallel connected to support the DC-bus voltage. The detailed wiring procedures are with:

- Connect DC-bus: TD1–TD3, TD5–TD6, and TE6–Bus-;
- Connect DC-bus capacitors: TD5–TD2, TD6–TE1, and TE2–Bus-;
- Connect phase lines: TB6–TB5, and TA6–TA5;
- Connect DC-source: Terminal Bus+ to DC positive, and Terminal Bus- to DC negative;
- Connect phase outputs: TA4 to Phase A, TB4 to Phase B, and TC4 to Phase C for three-phase PMSM;
- Connect the back EMF measurements: TB4–TA7, and TA4–N.

The vector control is usually adopted for the control of PMSM with torque regulation or speed regulation, and a structure of the vector control is illustrated in 12. In vector control, the three-phase currents are decoupled with $d-q$ currents, i_q and i_q, then i_q and i_q can be regulated individually through $d-q$ voltages, u_d and u_q. The coordinate transformations, e.g., Clarke, Park, inverse-Clarke, and inverse-Park transformations, play very important roles for the vector control, and more information about coordinate transformations can be found in [2]. Note that the rotor position angle is required for both Park and inverse-Park transformations. Though the embedded ABI incremental encoder of the PMSM and quadrature encoder pulse (QEP) decoder in the SYNDEM Kit can get the absolute rotor position, the position offset from initial rotor position should be compensated. A digital switch S_{iq} is used to selected either torque control mode and or speed control mode. If S_{iq} is with position 1, the torque control is enabled. For a surface mounted PMSM, there is a linear relationship between the electromagnetic torque T_e and the $q-$axis current i_q as $T_e = k_T i_q$, more information about this coefficient k_T can be found in [4]. The current reference i_q^* can be calculated through the torque reference as $i_q^* = \frac{T_e^*}{k_T}$. $d-$axis current reference i_d^* can be set as 0 to fulfill the maximum torque per ampere (MTPA) requirement. Through PI control of both $d-q$ currents, the voltage references, u_d and u_q, will be generated, and they can be converted to six space-vector pulse width modulation (SVPWM) signals to drive IGBT through both inverse-Park and inverse-Clarke transformations, and a SVPWM signal generator. If S_{iq} is with position 2, a PI control-based speed control loop is adopted to generated the current reference i_q^* for speed regulation. More information about the model of PMSM and vector control can be found in [4]. The main controller shown in Figure 12 with additional ADC measurements, QEP measurement, DAC output, and protection functions are implemented in Matalb/Simulink and directly downloaded to the TI C2000 TMS320F28335 ControlCARD for execution. A video of PMSM control based on the SYNDEM kit can be found in [5].

Case I: Rotor position offset calibration: As mentioned above, the rotor position offset from initial rotor position should be calibrated to compensate the direct measured rotor position from the encoder. Thanks to the DAC function of the SYNDEM kit, the waveforms of measured rotor position and the back EMF of the PMSM can be sent out simultaneously. Based on the characteristic of the PMSM, the initial rotor position of the PMSM is the intersection point of back EMF v_{ab} and v_{ca}, where the sign of signal $(v_{ab} - v_{ca})$ is from positive to negative at this point.

The initial rotor position can be calibrated with following procedures:

- Gets wire connected shown in Figure 11, where connections TB6–TB5 and TA6–TA5 should be disconnected to avoid the back EMF of the PMSM charging the DC-bus capacitors;
- Use the DC power supply to power the DC motor to drag the PMSM with the same rotation direction of the PMSM driving mode;
- Keep the PMSM rotating at a constant speed, e.g., around 833 rpm is considered in this test;
- Record waveforms of the measured rotor position and the back EMF on oscilloscope based on the DAC output, as shown in Figure 13.
- The initial rotor position can be achieved through record waveforms.

From Figure 13(a), it can be noticed that the speed of the PMSM is constant with the same amplitudes of the back EMF at each cycle. The zoomed-in results of measured rotor position and the back EMF are shown Figure 13(b), where rotor position offset can be calibrated with 145 degree based on the intersection point of back EMF v_{ab} and v_{ca} for this PMSM. The rotor position offset will be further updated in the vector control of the PMSM and implemented into the SYNDEM kit.

Case II: Torque control with current regulation: In this case, the torque control of the PMSM with current regulations is considered, and the experimental results are shown Figure 14(a). Initially the current references are set with $i_d^* = 0$ A, and $i_q^* = 0.5$ A, and control command is enabled at $t = 0.4$ s to regulated the currents. It can be noticed that the $d-$axis current i_d can be well regulated to zero, and $q-$axis current i_q starts to increase after control command and goes to steady-state after 0.8 s. Because the positive i_q provides positive electromagnetic torque T_e of the PMSM, the motor speed increases gradually and converges to steady-state with 280 rpm at about $t = 1.6$ s. The increase of motor speed usually will reduces the convergence rate of $q-$axis current i_q, because the effect of the back EMF. The convergence rate of the motor speed is affected by both the mechanical load and total system inertia. At $t = 2$ s, the $q-$axis current reference is changed to $i_q^* = 1$ A, and i_q can be regulated to its target after 0.8 s. The motor speed convenes to around 700 rpm at $t = 3.2$ s. The $d-$axis current i_d has slightly over-shoots and coverages to 0 A quickly. The over-shoots of i_d are caused by the coupled effects between the dynamics of both $d-$axis current i_d and $q-$axis current i_q. Therefore, the SYNDEM kit can provide torque control of the PMSM with accurate current regulation.

Case III: Motor speed control: In this case, the speed control of the PMSM is considered, and the experimental results are shown Figure 14(b). Initially motor speed reference is set with 500 rpm, and control command is enabled at $t = 0.4$ s to regulated the motor speed. Based on the speed control loop, the $q-$axis current reference i_q^*can be generated to drive the PMSM. Through the increase of the $q-$axis current i_q, the motor speed increases as well. Both motor speed and $q-$axis current can converge to steady-sate after about 1 s with 500 rpm of motor speed and $i_q = 0.7$ A. Compared to the Case of torque control with current regulation, the speed control usually can provide faster convergence of motor speed, but with slower convergence of motor current, because of different control targets. At $t = 2$ s, the motor speed reference is changed to 1000 rpm, the motor speed can be regulated to its target after 1s, and the $q-$axis current i_q converges to steady-state with $i_q = 1.3$ A simultaneously. Similar to Case II, the $d-$axis current i_d has slightly over-shoots because of the the coupled effects, it can coverage to 0 A quickly.

B. PV-battery System

During emergencies or natural disasters, the utility-grid might be damaged or not accessible, therefore, a sustainable electricity generation is critical for human survivals or other electricity needs. A PV-battery system, named "sustainable, portable, and efficient electricity delivery (SPEED) system", for emergency/disaster reliefs is presented by Texas Tech University (TTU) with standard utility AC output, as shown in 15. The detailed system design is shown in Fig. 16, where the SPEED system consists of a 180 W PV source, a 1.8 kWh battery pack, a SYNDEM Kit, and a data monitoring subsystem. The solar panels absorb solar energy and convert it into DC power. The battery pack is used for energy storage. The SYNDEM Kit provides the power electronic interface for both the PV source and the battery pack with standard utility AC output. The data monitoring subsystem is designed for monitoring and recording real-time data of the SPEED system through RS485 communication. To enhance the mechanical robustness and portability of the SPEED system, all hardware components, such as, the PV panels, the battery pack, the SYNDEM Kit, and the data monitoring subsystem, are mechanically mounted on a moving cart demonstrated in Fig. 15.

In the SPEED system, the SYNDEM Kit is configured as a DC-DC boost converter and a single-phase DC-AC converter, as shown in Fig. 17. The topology of the SPEED system is shown in Fig. 17(a), and the detailed configuration of the SYNDEM power converter is shown in Fig. 17(b). The detailed wiring procedures are with:

- Connect DC-bus: TD1–TD3, TD5–TD6, and TE6–Bus-;
- Connect DC-bus capacitors: TD5–TD2, and TE2–Bus-;
- Connect W-leg: TA1–TA3, TA5–TA6, TA1–TE1, and TA7–Bus-;
- Connect V-legs: TB6–N;

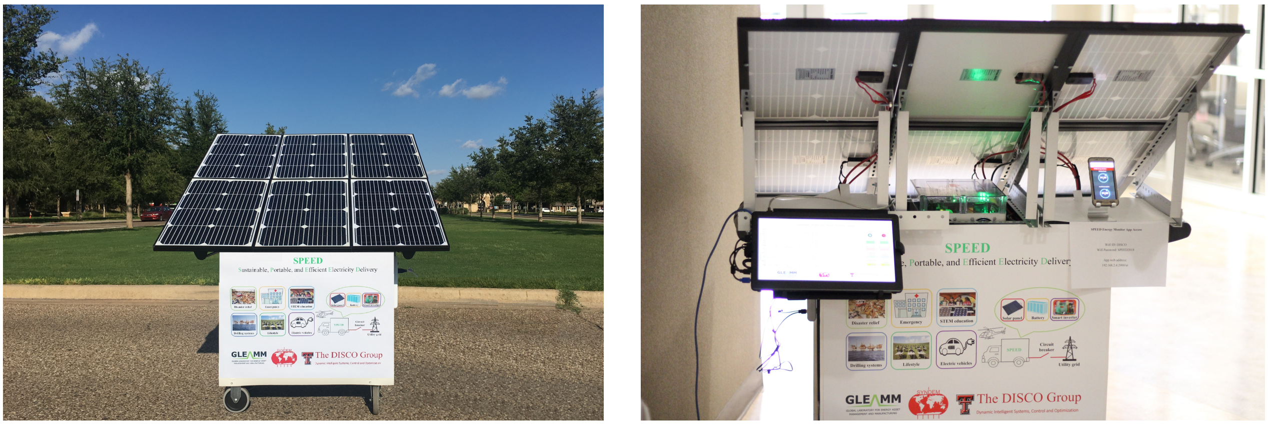

(a) Front view (b) Back view

Fig. 15. The SPEED system with both front view and back view

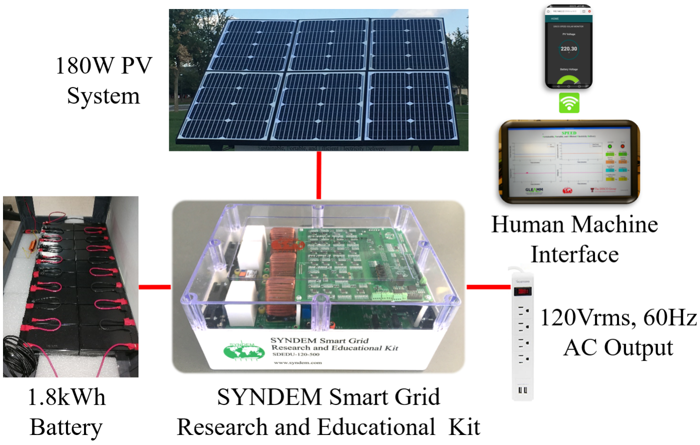

Fig. 16. The system design of the SPEED system

- Connect PV input: Terminal A to PV positive, and Terminal Bus- to PV ground;
- Connect the battery: Terminal Bus+ to Battery positive, and Terminal Bus- to Battery negative;
- Connect AC output: TC2 to load hot, and Terminal N to load neutral
- Connect utility-grid: Terminal C to grid hot, and Terminal N to grid neutral.

While the DC-DC boost converter converts DC power from the PV source into the battery pack, and the single-phase DC-AC converter feeds the DC power from both the PV source and the battery pack into AC load or AC grid. The main functions of the SPEED system include islanded mode operation with the grid-forming capability for outdoor activities of emergency/disaster reliefs, and grid-connected mode operation for energy harvesting at normal scenarios, where the energy generated by the PV source can be sent to the utility-grid with the maximum power acquisition of PV source. Advanced power electronics control technologies are developed and embedded into the TI C2000 TMS320F28335 ControlCARD to control the both the DC-DC boost converter and the DC-AC converter. For example, the robust droop control technology [6] is adopted for islanded operation of the SPEED system, and extremum-seeking (ES)-based maximum power point tracking (MPPT) for maximum power acquisition of the PV source and robust grid-integration technology for the DC-AC converter can be found in [7]. Furthermore, a video for the field test of the SPEED system conducted on TTU campus can be found in [8].

Results: Though the SPEED system has different working modes, the grid-connected operation of the SPEED system is selected and demonstrated in the article, as shown in Fig. 18. When the system is connected to the utility-grid, grid-connected operation is automatically triggered. After the system starting, the PV power increases to the maximum value, around 160 W quickly, due to the fast convergence of the ES-based MPPT, as shown in Fig. 18(a). The changes of the PV power are caused by the varying sunlight conditions and the changes of the PV temperature. During $t = 8$ minute to $t = 18$ minute, there are large variances in PV power, due to the PV shading effect from the moving clouds. The PV shading also affects the PV voltage, as shown in Fig. 18(b), and there is a large voltage drop around $t = 17.5$ minute with the fully blocked sunlight. The grid real power follows the trend of PV power well, as shown Fig. 18(c). The grid real power is slightly smaller than PV power after $t = 2$ minute, because

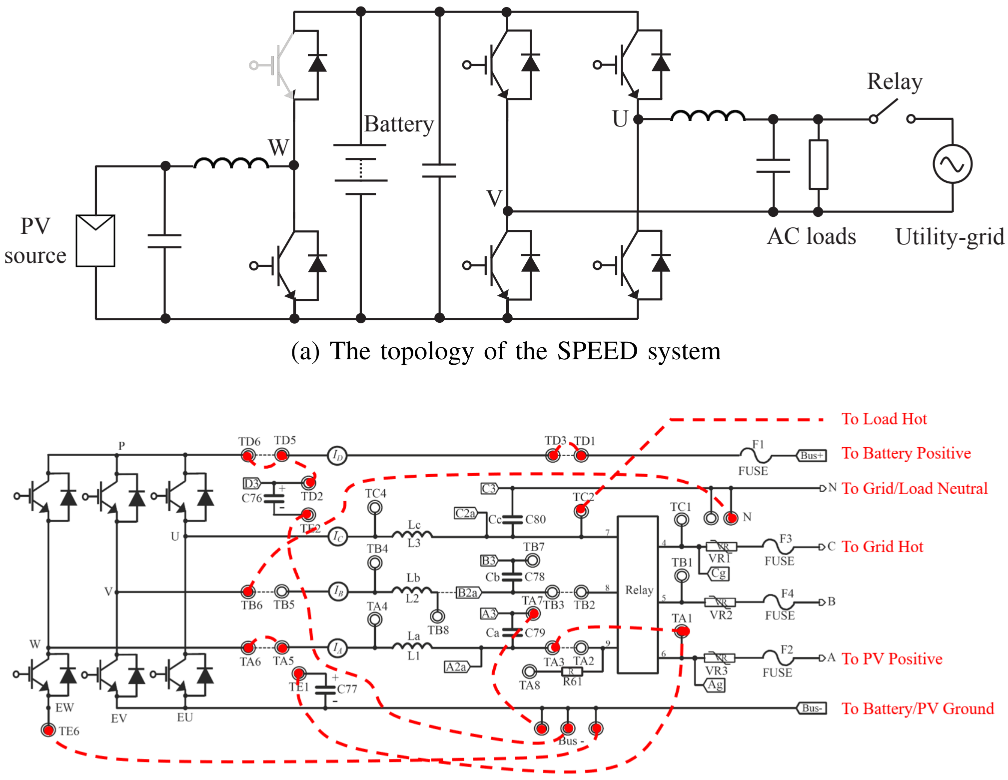

(a) The topology of the SPEED system

(b) The configuration of the SYNDEM power converter

Fig. 17. The configuration of the SYNDEM power converter as a DC-DC boost converter and a DC-AC converter

of the system efficiency. In grid-connected mode, the battery voltage is kept balance with a almost constant value as shown in Fig. 18(f), and battery power is almost kept around zero in steady-state (after $t = 2$ minute) as shown in Fig. 18(e). Almost all power generated by the PV source are sent to utility-grid during grid-connected operation. Before $t = 2$ minute,the negative battery power at initial state is because that the DC/AC controller is enabled after DC/DC controller, and there is a very short-term of the battery charging. The grid reactive power is always regulated around 0 Var to keep the unity power factor, as shown in Fig. 18(g). The reasons for small spikes of both grid real power and grid reactive power are from different aspects, e.g., the measurement noises, the small disturbances for both grid voltage and grid frequency. It can be noticed that both grid voltage and grid frequency are varying, as shown in Fig. 18(d) and Fig. 18(h), because there is a high penetration of renewables in Texas utility-grid. Therefore, the SYNDEM kit can provide robust grid-control operation of this PV-storage SPEED system.

IV. Conclusions

In this paper, the SYNDEM Smart Grid Research and Educational Kit, which is a reconfigurable, open-source, multifunctional power electronic converter with the capability of directly downloading codes from Matlab/Simulink, is introduced with the aim of helping researchers, graduate students, and engineers remove the barriers to go real from simulations to experiments for various power electronic-based systems. This removes two major challenges, i.e., the lack of suitable hardware platforms and the burden of software coding, faced by the control community in carrying out experiments for power and energy systems. This makes it possible to quickly obtain experimental results after completing simulations. The kit is expected to maximize the strengths of the control community in developing control algorithms and minimize the efforts on developing hardware systems and programming the algorithms, which will significantly improve the efficiency and productivity of research and learning. The kit can be adopted for lab-bench systems as well as standalone research projects. While the kit is developed for power and energy related applications, it can be applied to the research and education of other control systems as well because of its versatile interfaces and computational power.

References

[1] Q.-C. Zhong, *Power Electronics-Enabled Autonomous Power Systems: Next Generation Smart Grids*. Wiley-IEEE Press, 2017.

[2] Q.-C. Zhong and T. Hornik, *Control of Power Inverters in Renewable Energy and Smart Grid Integration*. Wiley-IEEE Press, 2013.

[3] Q. Zhong and W. Ming, “A θ-Converter that reduces common mode currents, output voltage ripples, and total capacitance required,” *IEEE Trans. Power Electron.*, vol. 31, no. 12, pp. 8435–8447, Dec. 2016.

[4] B. Ren, Y. Wang, and Q.-C. Zhong, “UDE-based control of variable-speed wind turbine systems,” *International Journal of Control*, vol. 90, no. 1, pp. 121–136, 2017.

[5] Go real: Power electronics from simulations to experiments in hours–motor drive case studies. https://www.youtube.com/watch?v=LlpzpH8Aai8.

[6] Q.-C. Zhong, Y. Wang, and B. Ren, “UDE-based robust droop control of inverters in parallel operation,” *IEEE Trans. Ind. Electron.*, vol. 64, no. 9, pp. 7552–7562, Sept. 2017.

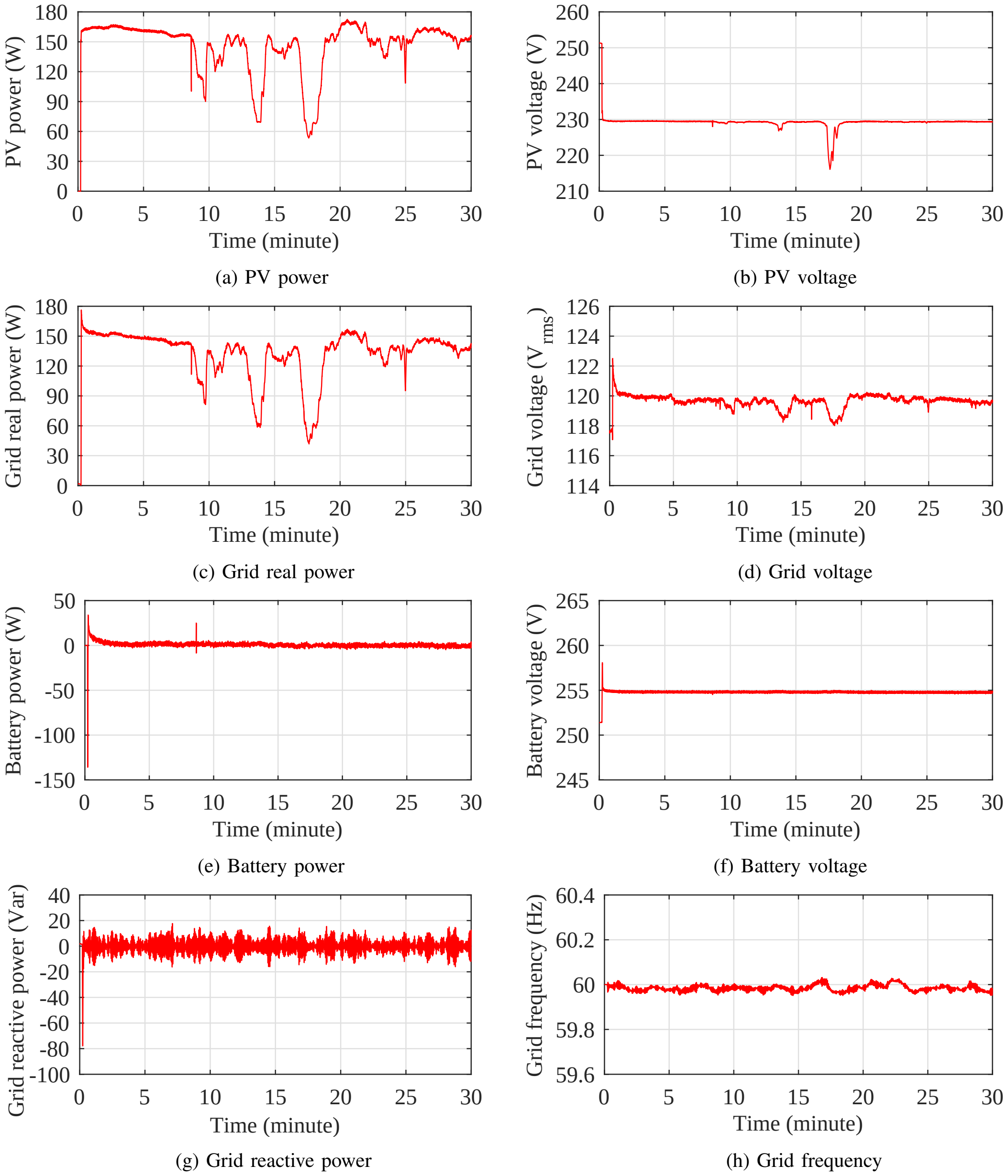

(a) PV power (b) PV voltage (c) Grid real power (d) Grid voltage (e) Battery power (f) Battery voltage (g) Grid reactive power (h) Grid frequency

Fig. 18. Grid-connected operation of the SPEED system

[7] Y. Wang and B. Ren, "Fault ride-through enhancement for grid-tied PV systems with robust control," *IEEE Trans. Ind. Electron.*, vol. 65, no. 3, pp. 2302–2312, Mar. 2018.

[8] Sustainable, portable, and efficient electricity delivery (SPEED)_prototype v2.0. https://www.youtube.com/watch?time_continue=10&v=uVcM5kwRhQ0.